SCIENCE CHINA
Information Sciences

• RESEARCH PAPER •

December 2021, Vol. 64 222303:1–222303:11
https://doi.org/10.1007/s11432-020-3048-9

Directional modulation with distributed receiver selection for secure wireless communications

Hongyan ZHANG[1], Yue XIAO[1*], Wanbin TANG[1*], Gang WU[1], Hong NIU[1] & Xiaotian ZHOU[2]

[1]*National Key Laboratory of Science and Technology on Communications, University of Electronic Science and Technology of China, Chengdu* 611731*, China;*
[2]*Science and Technology on Communication Networks Laboratory, The 54th Research Institute of China Electronics Technology Group Corporation, Shijiazhuang* 050081*, China*

Received 25 March 2020/Revised 25 June 2020/Accepted 26 August 2020/Published online 24 November 2021

Abstract In this paper, a novel directional modulation with distributed receiver selection (DM-DRS) scheme is proposed for secure wireless communications. In DM-DRS, a particular subset of receivers is activated and part of the information bits are modulated by the index of the activation pattern, in addition to traditional digital modulation. Especially, the scrambling matrix is introduced for the sake of preventing the eavesdropping. Moreover, the performances of bit error rate (BER) in terms of the union bound for both the legitimate user and eavesdropper are respectively derived in the context of an optimal joint maximum likelihood (ML) detector, and the theoretical BER upper bounds are demonstrated to be tight by the numerical results. In the context of the discrete-input and continuous-output system, the ergodic secrecy rates of the legitimate user and the eavesdropper are obtained, the secrecy rate is also quantified. Furthermore, our numerical results exhibit that DM-DRS can achieve an increased transmission rate compared to its traditional directional modulation with cooperative receivers (DM-CR) and spatial and direction modulation (SDM) counterparts, while guaranteeing an improved BER performance.

Keywords directional modulation, distributed receiver selection, bit error rate, secrecy rate

Citation Zhang H Y, Xiao Y, Tang W B, et al. Directional modulation with distributed receiver selection for secure wireless communications. Sci China Inf Sci, 2021, 64(12): 222303, https://doi.org/10.1007/s11432-020-3048-9

1 Introduction

Since the broadcasting property of the wireless propagation medium makes the transmitted information vulnerable to the interception by the eavesdropper, the security of information is gradually threatened so that wireless communication faces more and more safety challenges [1]. Unlike traditional high-layer encryption methods, where the heavy-computation processes are required, much more attention has been paid to the secure transmission of the physical layer (PHY) [2, 3]. Especially, there are a variety of techniques for achieving PHY security communication, such as jamming, beam-steering, and their combinations [4]. The key idea of the above-mentioned technology is to take advantage of the characteristics of wireless channels to deliver the legitimate information to the intended user, while maintaining the information confidential to the eavesdropper.

Directional modulation (DM) [5–12], as one of the promising techniques offering PHY security, is capable of permitting the transmitted signal to be correctly received at the desired direction, while simultaneously scrambling the undesirable directions. Particularly, in [7], the fundamental concept of DM was first introduced for synthesizing the directional signals at the near-field full antenna level. In [8], an improved DM was developed, and the full antenna array is introduced to steer the main beam towards the desired direction so that the maximum power will ensure the reliable reception in the main-lobe direction, while information leakage may still occur in the side-lobe direction. In [9], a low-complexity and antenna-level antenna subset modulation (ASM) technique was proposed, in contrast to the full antenna

* Corresponding author (email: xiaoyue@uestc.edu.cn, wbtang@uestc.edu.cn)

array, the improvement of security performance relies on activating a subset of transmission antennas with the aid of inter-antenna phase shift. However, the aforementioned radio frequency (RF)-based synthesis methods [7–9] focused on signaling on the RF frontend at the cost of high operational complexity. In order to alleviate this problem, DM baseband synthesis methods [10–12] have offered reduced-complexity applications in secure communication systems. Specifically, in [10], the authors proposed a silent antenna hopping (SAH) scheme, where the DM characteristic is achieved by randomly switching. In [11], the authors introduced an orthogonal vector approach for allowing analysis and synthesis of digital DM signal with only one transmission data stream under the dynamic and static scenarios. The further improved approach was developed in [12], where the multi-beam DM baseband signals were synthesized based on the artificial noise. However, one of the major drawbacks of the above-mentioned DM methods lies in that the DM signal may fail to guarantee information security, when the eavesdropper and the legitimate user are located along an identical direction.

To address this issue, a class of improved DM methods with the aid of distributed receivers were designed. More specially, directional modulation with cooperative receivers (DM-CR) was developed in [13] employing multiple distributed receivers for efficiently preventing eavesdropping, even if the eavesdropper and the legitimate receiver share the same transmission direction. Nevertheless, DM-CR is with low transmission rate, since only traditional amplitude phase modulation (APM) is considered. To circumvent this problem, an improved spatial and directional modulation (SDM) with scrambling was developed in [14] where only one single-antenna receiver is employed at the eavesdropper. In SDM, the concept of spatial modulation (SM) [15–17] is introduced into traditional DM systems, which can transmit extra information by activating one of the distributed receivers. That is, through combining the advantages of SM and DM, the previously proposed SDM not only improves the transmission efficiency, but also enhances the security. However, there still exists a limitation that only one receiver is activated for communication by the legitimate user, and only the traditional APM symbol is detected by the eavesdropper. Additionally, despite the union bound approach of bit error rate (BER) has been analyzed both in DM-CR and SDM systems, the secrecy rate analysis has not been quantified for characterizing the performance of these systems.

Against this background, in this paper, we introduce the concept of receiver subset selection [18–20] into distributed DM systems. Namely, the proposed directional modulation with the distributed receiver selection (DM-DRS) scheme aims at bringing higher transmission rate, while guaranteeing improved secure transmission performance. To elaborate a little further, as traditional DM-CR and SDM schemes, the DM characteristics are achieved by introducing the scrambling matrix into the DM-DRS scheme. Note that the scrambling matrix is known at both the transmitter and the legitimate user, but unknown at the eavesdropper, it guarantees the system security. As for the transmission rate, on the one hand, there is no extra index information transmitted by the activated receiver in traditional DM-CR, and the extra index information is conveyed by only one activated receiver in traditional SDM. By contrast, the receiver subset selection is employed by activating multiple distributed receivers, while exploiting the index combination of the distribution receivers to convey extra information in the proposed DM-DRS scheme. On the other hand, only one information data stream can be transmitted by APM symbols in traditional DM-CR and SDM schemes, whereas the transmission of multiple data streams can be simultaneously achieved in the proposed DM-DRS. Therefore, the proposed scheme can effectively improve the transmission rate compared to DM-CR and SDM schemes, in addition to achieving secure transmission. The main contributions of this paper can be summarized as follows.

(1) The system model of the proposed DM-DRS is described in detail, where the distributed receivers are connected with the aid of optical fibers. In order to enhance the security, the beamforming vector is designed to preserve its power in the desired direction, which aims at scrambling the amplitude of the signal observed at the eavesdropper when the direction of the legitimate user is different from that of the eavesdropper. At the same time, the scrambling matrix is further introduced to scramble the phase of the signal observed at the eavesdropper. Consequently, both the amplitude and phase of the symbols received at the eavesdropper are scrambled in the proposed DM-DRS scheme. Simultaneously, through using the receiver subset selection, not only the information is transmitted by the index of the activation pattern, but also the multiple receivers are activated to transmit the multiple traditional APM symbols, then it has the advantage of increasing the transmission rate. Furthermore, compared with traditional DM-CR and SDM, it is more difficult for the eavesdropper to decode the index of the receiver subset selection in the proposed DM-DRS scheme. More specially, since multiple APM symbols are conveyed on the activated receivers, and the corresponding multiple scrambling factors effectively make an impact

on these APM symbols, it is capable of improving the security performance.

(2) Theoretical analysis of average bit error probability (ABEP) union bound for the legitimate user and eavesdropper are respectively derived, when an optimal joint maximum likelihood (ML) detector is employed, and then the secrecy rate of the proposed DM-DRS is quantified in the worst case that the scrambling matrix is known at the eavesdropper.

(3) The numerical results demonstrate that the DM-DRS scheme outperforms its traditional DM-CR [13] and SDM [14] counterparts in terms of BER performance and transmission rate. On the other hand, both the legitimate user and eavesdropper are capable of achieving the ergodic rate upper bound when the signal-to-noise ratio (SNR) is sufficiently high, and when compares to traditional DM-CR and SDM schemes, the proposed DM-DRS also can achieve the best secrecy rate performance in the low and medium SNR regions. Furthermore, the fewer the eavesdropper's distributed receivers are, the larger the SNR interval to attain a positive secrecy rate will be.

The remainder of this paper is organized as follows. In Section 2, the system is described, including the designs of beamforming, signaling and signal detection. In Section 3, the theoretical analysis of ABEP union bound for the legitimate user and the eavesdropper is respectively derived, and the secrecy rate of the proposed DM-DRS is characterized. Furthermore, our numerical results are provided in Section 4, before concluding in Section 5.

Notation. Throughout this paper, bold upper case represents matrix and bold lower case represents vector. $(\cdot)^{\mathrm{H}}$, $|\cdot|$, $\|\cdot\|$ and $\Re(\cdot)$ represent the conjugate transpose, the cardinality of a set, the Frobenius norm and real operators, respectively. Furthermore, $\binom{N_r}{N_u}$ represents the number of ways of selecting N_u outcomes from N_r possibilities, $\lfloor\cdot\rfloor$ and $Q(\cdot)$ represent floor function and Gaussian Q-function, respectively. Finally, $\mathcal{CN}(\cdot,\cdot)$ represents circularly symmetric complex Gaussian distribution.

2 Proposed DM-DRS systems

2.1 System description

Let us consider that the transmitter (Alice) equipped with N_t antennas communicates with the legitimate user (Bob), equipped with N_r distributed single-antenna receivers, and these receivers are located along different directions, connecting with each other by optical fibers. Moreover, the number of active receivers activated to receive the signal is N_u, and hence the feasible number of combinations to select N_u out of N_r receivers will be given by $\binom{N_r}{N_u}$. For the convenience of information mapping, the number of combinations will be the power of two, and then the number of the permitted receiver subset combinations is $f = 2^{\lfloor \log_2 \binom{N_r}{N_u} \rfloor}$. Hence, the transmit information can determine the index of the selected receiver subset, which will carry $k_1 = \log_2 f$ bits. Note that, in addition to the partial information transmitted by the index of the selected receiver subset, since N_u receivers are selected and one APM symbol is conveyed by each receiver, the other part is conveyed by traditional APM symbols as $k_2 = N_u \times \log_2 M$ bits, where M is the modulation order. As a result, one block of $k_1 + k_2$ bits composes a DM-DRS super symbol, and thus the transmission rate is effectively improved. On the other hand, an eavesdropper Eve having N_e distributed single-antenna receivers is also assumed, which is passively eavesdropping the legitimate signals.

2.2 Beamforming design

For the sake of simplicity, we assume that Alice is equipped with uniform linear phased array, where the antennas are located at the geometric center. Consequently, channel vector $\boldsymbol{h}^{\mathrm{H}}(\theta)$ for a receiver at the directional angle θ is given by

$$\boldsymbol{h}^{\mathrm{H}}(\theta) = \left[\mathrm{e}^{-\mathrm{j}\left(\frac{N_t-1}{2}\right)\frac{2\pi}{\lambda}d\cos\theta}, \mathrm{e}^{-\mathrm{j}\left(\frac{N_t-1}{2}-1\right)\frac{2\pi}{\lambda}d\cos\theta}, \ldots, \mathrm{e}^{\mathrm{j}\left(\frac{N_t-1}{2}\right)\frac{2\pi}{\lambda}d\cos\theta}\right], \tag{1}$$

where λ represents the wavelength, $d \leqslant \lambda/2$ is the antenna spacing of the phased array at Alice. Assuming that the channel from Alice to Bob experiences free space, the channel matrix $\boldsymbol{H}(\Theta_B) \in \mathbb{C}^{N_r \times N_t}$ can be formulated as

$$\boldsymbol{H}(\Theta_B) = [\boldsymbol{h}(\theta_1), \boldsymbol{h}(\theta_2), \ldots, \boldsymbol{h}(\theta_{N_r})]^{\mathrm{H}}, \tag{2}$$

where $\Theta_B = \{\theta_1, \theta_2, \ldots, \theta_{N_r}\}$ is the direction set of Bob, $\boldsymbol{h}(\theta_i), i = 1, 2, \ldots, N_r$ represents the channel vector between Alice and Bob's ith receiver at direction θ_i.

Additionally, in order to guarantee transmission security, the beamforming vector is designed to preserve its power at the desired direction. Therefore, for Bob's ith receiver, its corresponding beamforming vector $\boldsymbol{w}_i$ is given by

$$\boldsymbol{w}_i = \boldsymbol{h}(\theta_i)/N_t. \tag{3}$$

When considering all the receivers, the beamforming matrix $\boldsymbol{W} \in \mathbb{C}^{N_t \times N_r}$ can be expressed as

$$\boldsymbol{W} = [\boldsymbol{w}_1, \boldsymbol{w}_2, \ldots, \boldsymbol{w}_{N_r}]. \tag{4}$$

2.3 Signaling and detection

As mentioned before, DM-DRS modulates the incoming bit streams into one block of $k_1 + k_2$ bits, where the initial k_1 bits are employed to select the set of activated receivers. To represent simply, after obtaining the set, we select the column vectors at the corresponding positions from the identity matrix $\mathbf{I}_{N_r \times N_r}$. Namely, the initial k_1 bits can be transmitted by the index of the identity column vector subset. Meanwhile, for each selected identity column vector $\boldsymbol{e}_i$, the APM symbol b_m will be transmitted, where $b_m \in \mathcal{B} = \{b_1, b_2, \ldots, b_M\}$, for carrying the last k_2 bits.

For example, if the incoming bit streams are divided into one block of 6 ($k_1 + k_2$=6) bits, and Bob is equipped with 4 ($N_r = 4$) cooperative single-antenna receivers, the number of actived receivers is 2 ($N_u = 2$), so that $k_1 = 2$. According to the initial 2 bits, we select two corresponding column vectors (e.g., $\boldsymbol{e}_1, \boldsymbol{e}_2$) from $\mathbf{I}_{N_r \times N_r}$. Simultaneously, for each column vector, the APM symbol is transmitted. According to the residual 4 ($k_2 = 4$) bits, we select two corresponding APM signals (e.g., b_1, b_2) from $\mathcal{B}$. So the transmitted signal is $\boldsymbol{e}_1 b_1 + \boldsymbol{e}_2 b_2$, also expressed as $[\boldsymbol{e}_1 \boldsymbol{e}_2]\left[\begin{smallmatrix} b_1 \\ b_2 \end{smallmatrix}\right]$.

In general, according to the selected N_u column vectors, Alice directs the N_u beams toward the receivers to transmit APM symbols, and thus Alice generates a symbol vector $\boldsymbol{x}_{l,s}$, which is expressed as

$$\boldsymbol{x}_{l,s} = \mathbf{I}_l \boldsymbol{b}_s, \tag{5}$$

where $\mathbf{I}_l, l = 1, 2, \ldots, 2^{k_1}$ represents a matrix formed through the N_u selected column vectors from the identity matrix $\mathbf{I}_{N_r \times N_r}$. In addition, $\boldsymbol{b}_s, s = 1, 2, \ldots, 2^{k_2}$ represents a column vector, formed through the N_u selected APM symbols from $\mathcal{B}$. Note that, these APM symbols may also employ different modulation orders.

Specially, in order to enhance the system security, a scrambling matrix will be introduced into the DM-DRS system, which is known at Bob, but unknown at Eve. Therefore, the scrambling matrix is capable of deteriorating Eve's detection without degrading BER performance of Bob. Consequently, the transmitted signal at Alice is

$$\boldsymbol{s}_{l,s} = \boldsymbol{W} \boldsymbol{\Lambda} \boldsymbol{x}_{l,s}, \tag{6}$$

where $\boldsymbol{\Lambda} = \operatorname{diag}\{\lambda_1, \lambda_2, \ldots, \lambda_{N_r}\} \in \mathbb{C}^{N_r \times N_r}$ represents the scrambling matrix, and $\lambda_i = \mathrm{e}^{\mathrm{j}\varphi_i}, i = 1, 2, \ldots, N_r$ is corresponding to Bob's ith legitimate receiver. Note that, the scrambling factor is consistent with [13], which brings the benefit of phase scrambling, and thus the scrambling factor cannot be set to be too small for efficient phase scrambling. Moreover, for the sake of improving the transmission security, we may set different scrambling factors to avoid the case that Eve tries to eavesdrop the scrambling factor of one of the receivers. Furthermore, owing to the introduction of the receiver subset selection, the multiple APM symbols are transmitted and the corresponding multiple scrambling factors make an effective impact on these APM symbols, and thus the transmission security can be guaranteed. Peculiarly, the scrambling matrix is updated at the symbol rate, which further prevents eavesdropping from the passive Eve, such that the transmission security is to be improved.

Under the assumption of a free space channel environment, the received signals at Bob and Eve are, respectively, obtained as

$$\boldsymbol{r}_B = \boldsymbol{H}\left(\Theta_B\right) \boldsymbol{s}_{l,s} + \boldsymbol{n} = \boldsymbol{H}\left(\Theta_B\right) \boldsymbol{W} \boldsymbol{\Lambda} \boldsymbol{x}_{l,s} + \boldsymbol{n}, \tag{7}$$

and

$$\boldsymbol{r}_E = \boldsymbol{H}(\Theta_E) \boldsymbol{s}_{l,s} + \boldsymbol{n}_E = \boldsymbol{H}(\Theta_E) \boldsymbol{W} \boldsymbol{\Lambda} \boldsymbol{x}_{l,s} + \boldsymbol{n}_E, \tag{8}$$

where $\boldsymbol{H}\left(\Theta_E\right) \in \mathbb{C}^{N_e \times N_t}$ is Eve's channel matrix and $\Theta_E = \{\theta_1, \theta_2, \ldots, \theta_{N_e}\}$ is the direction set of Eve, $\boldsymbol{n}$ is the circularly symmetric complex Gaussian noise vector with zero mean and covariance matrix

$\sigma_n^2\mathbf{I}_{N_r\times N_r}$, represented as $\boldsymbol{n}\sim\mathcal{CN}\left(\mathbf{0},\sigma_n^2\mathbf{I}_{N_r\times N_r}\right)$, and $\boldsymbol{n}_E$ is also the circularly symmetric complex Gaussian noise with $\boldsymbol{n}_E\sim\mathcal{CN}\left(\mathbf{0},\sigma_E^2\mathbf{I}_{N_e\times N_e}\right)$. Note that, according to [13], each of the diagonal elements of $\boldsymbol{H}\left(\Theta_B\right)\boldsymbol{W}$ is equal to 1 and that of $\boldsymbol{H}\left(\Theta_E\right)\boldsymbol{W}$ is less than or equal to 1, and the amplitude or power of Eve's received symbols is reduced. Furthermore, owing to the introduction of $\boldsymbol{\Lambda}$, it is capable of scrambling the phase of Eve's received symbols.

Based on (7), the optimal detector for Bob is the ML one that jointly decodes the identity column vector combination l and modulation symbol combination s, written as

$$\left\langle\hat{l},\hat{s}\right\rangle=\arg\min_{\boldsymbol{x}_{l,s}\in\mathcal{X}}\left\{\left\|\boldsymbol{r}_B-\boldsymbol{H}\left(\Theta_B\right)\boldsymbol{W}\boldsymbol{\Lambda}\boldsymbol{x}_{l,s}\right\|^2\right\},\tag{9}$$

where $\mathcal{X}$ is a set containing all the possible DM-DRS super symbols. From (7) and (9), we can see that Bob is capable of recovering the transmitted signal, and further decoding the corresponding initial k_1 bits and the last k_2 bits.

For Eve, the channel state information may be obtained, and then the beamforming matrix can be obtained. Nevertheless, the scrambling matrix may be difficult to know. Thus, Eve carries out the optimal ML detection as

$$\left\langle\hat{l},\hat{s}\right\rangle=\arg\min_{\boldsymbol{x}_{l,s}\in\mathcal{X}}\left\{\left\|\boldsymbol{r}_E-\boldsymbol{H}\left(\Theta_E\right)\boldsymbol{W}\boldsymbol{x}_{l,s}\right\|^2\right\}.\tag{10}$$

In DM-DRS, only part of the distributed receivers are activated according to the delivered information on each transmission. This part of information modulated by the index of the activation pattern is difficult to be obtained at Eve. On the other hand, based on (8) and (10), owing to the introduction of scrambling matrix, the detection performance of the APM symbols at Eve will be seriously degraded. Namely, Eve is difficult to recover the last k_2 bits, in addition to the initial k_1 bits. Consequently, as shown in Section 4, Eve's BER performance is significantly degraded, even if Eve is located along the same direction as one of Bob's receivers like in [13, 14].

3 Performance analysis

In this section, in order to derive the theoretical ABEP for Bob and Eve, the union bound approach [18] is introduced. Moreover, the secrecy rate is also investigated in the context of discrete-input and continuous-output signalling.

3.1 ABEP analysis

3.1.1 *ABEP analysis at Bob*

Based on the assumption of the ML detection in (9), Bob's ABEP union bound can be obtained as

$$P_B\leqslant\frac{1}{|\mathcal{X}|\log_2|\mathcal{X}|}\sum_{\boldsymbol{x}_{l,s}\in\mathcal{X}}\sum_{\substack{\boldsymbol{x}_{u,v}\in\mathcal{X}\\ \boldsymbol{x}_{u,v}\neq\boldsymbol{x}_{l,s}}}e(\boldsymbol{x}_{l,s},\boldsymbol{x}_{u,v})P(\boldsymbol{x}_{l,s}\to\boldsymbol{x}_{u,v}),\tag{11}$$

where $e(\boldsymbol{x}_{l,s},\boldsymbol{x}_{u,v})$ is the number of the different bits between the equivalent bit representations of $\boldsymbol{x}_{l,s}$ and $\boldsymbol{x}_{u,v}$, $P(\boldsymbol{x}_{l,s}\to\boldsymbol{x}_{u,v})$ is the pairwise error probability (PEP).

Particularly, the PEP in (11) is equal to

$$\begin{aligned}P(\boldsymbol{x}_{l,s}\to\boldsymbol{x}_{u,v})&=P(\left\|\boldsymbol{r}_B-\boldsymbol{H}_{\boldsymbol{\Lambda}}\boldsymbol{x}_{l,s}\right\|^2>\left\|\boldsymbol{r}_B-\boldsymbol{H}_{\boldsymbol{\Lambda}}\boldsymbol{x}_{u,v}\right\|^2)\\&=P(\left\|\boldsymbol{H}_{\boldsymbol{\Lambda}}\boldsymbol{x}_{l,s}+\boldsymbol{n}-\boldsymbol{H}_{\boldsymbol{\Lambda}}\boldsymbol{x}_{l,s}\right\|^2>\left\|\boldsymbol{H}_{\boldsymbol{\Lambda}}\boldsymbol{x}_{l,s}+\boldsymbol{n}-\boldsymbol{H}_{\boldsymbol{\Lambda}}\boldsymbol{x}_{u,v}\right\|^2)\\&=P\left\{\Re\left[\boldsymbol{n}^{\mathrm{H}}(\boldsymbol{H}_{\boldsymbol{\Lambda}}\boldsymbol{x}_{u,v}-\boldsymbol{H}_{\boldsymbol{\Lambda}}\boldsymbol{x}_{l,s})\right]>\frac{1}{2}\left\|\boldsymbol{H}_{\boldsymbol{\Lambda}}\boldsymbol{x}_{u,v}-\boldsymbol{H}_{\boldsymbol{\Lambda}}\boldsymbol{x}_{l,s}\right\|^2\right\},\end{aligned}\tag{12}$$

where we define $\boldsymbol{H}_{\boldsymbol{\Lambda}}=\boldsymbol{H}\left(\Theta_B\right)\boldsymbol{W}\boldsymbol{\Lambda}$.

Since $\Re[\boldsymbol{n}^{\mathrm{H}}(\boldsymbol{H}_{\boldsymbol{\Lambda}}\boldsymbol{x}_{u,v}-\boldsymbol{H}_{\boldsymbol{\Lambda}}\boldsymbol{x}_{l,s})]$ is a real Gaussian random variable, which obeys the distribution of $\mathcal{CN}(0,\frac{\sigma_n^2}{2}\left\|\boldsymbol{H}_{\boldsymbol{\Lambda}}\boldsymbol{x}_{u,v}-\boldsymbol{H}_{\boldsymbol{\Lambda}}\boldsymbol{x}_{l,s}\right\|^2)$, the PEP can be derived as

$$P(\boldsymbol{x}_{l,s}\to\boldsymbol{x}_{u,v})=Q\left(\sqrt{\frac{\left\|\boldsymbol{H}_{\boldsymbol{\Lambda}}(\boldsymbol{x}_{u,v}-\boldsymbol{x}_{l,s})\right\|^2}{2\sigma_n^2}}\right).\tag{13}$$

As a result, the union bound of Bob's ABEP can be obtained by substituting (13) into (11).

3.1.2 *ABEP analysis at Eve*

Similarly, based on the joint ML detection of (10), Eve's ABEP union bound can be given by

$$P_E \leqslant \frac{1}{|\mathcal{X}|\log_2|\mathcal{X}|}\sum_{\boldsymbol{x}_{l,s}\in\mathcal{X}}\sum_{\substack{\boldsymbol{x}_{u,v}\in\mathcal{X}\\ \boldsymbol{x}_{u,v}\neq\boldsymbol{x}_{l,s}}} e(\boldsymbol{x}_{l,s},\boldsymbol{x}_{u,v})P_{\boldsymbol{H}(\Theta_E)}(\boldsymbol{x}_{l,s}\to\boldsymbol{x}_{u,v}), \tag{14}$$

where $P_{\boldsymbol{H}(\Theta_E)}(\boldsymbol{x}_{l,s}\to\boldsymbol{x}_{u,v})$ is the PEP for a given Eve's channel matrix $\boldsymbol{H}(\Theta_E)$, and the PEP can be further formulated as

$$\begin{aligned}
&P_{\boldsymbol{H}(\Theta_E)}(\boldsymbol{x}_{l,s}\to\boldsymbol{x}_{u,v})\\
&=P\left(\|\boldsymbol{r}_E-\boldsymbol{G}\boldsymbol{x}_{l,s}\|^2>\|\boldsymbol{r}_E-\boldsymbol{G}\boldsymbol{x}_{u,v}\|^2\right)\\
&=P\left(\|\boldsymbol{G}\boldsymbol{\Lambda}\boldsymbol{x}_{l,s}+\boldsymbol{n}_E-\boldsymbol{G}\boldsymbol{x}_{l,s}\|^2>\|\boldsymbol{G}\boldsymbol{\Lambda}\boldsymbol{x}_{l,s}+\boldsymbol{n}_E-\boldsymbol{G}\boldsymbol{x}_{u,v}\|^2\right)\\
&=P\left\{\Re\left[{\boldsymbol{n}_E}^{\mathrm{H}}(\boldsymbol{G}\boldsymbol{x}_{u,v}-\boldsymbol{G}\boldsymbol{x}_{l,s})\right]>\frac{\|\boldsymbol{G}\boldsymbol{\Lambda}\boldsymbol{x}_{l,s}-\boldsymbol{G}\boldsymbol{x}_{u,v}\|^2-\|\boldsymbol{G}\boldsymbol{\Lambda}\boldsymbol{x}_{l,s}-\boldsymbol{G}\boldsymbol{x}_{l,s}\|^2}{2}\right\},
\end{aligned} \tag{15}$$

where $\boldsymbol{G}=\boldsymbol{H}(\Theta_E)\boldsymbol{W}$.

Furthermore, $\Re[{\boldsymbol{n}_E}^{\mathrm{H}}(\boldsymbol{G}\boldsymbol{x}_{u,v}-\boldsymbol{G}\boldsymbol{x}_{l,s})]$ is with the distribution of $\mathcal{CN}(0,\frac{\sigma_E^2\|\boldsymbol{G}\boldsymbol{x}_{u,v}-\boldsymbol{G}\boldsymbol{x}_{l,s}\|^2}{2})$, and then, the PEP can be represented as

$$P_{\boldsymbol{H}(\Theta_E)}(\boldsymbol{x}_{l,s}\to\boldsymbol{x}_{u,v})=Q\left(\frac{\|\boldsymbol{G}\boldsymbol{\Lambda}\boldsymbol{x}_{l,s}-\boldsymbol{G}\boldsymbol{x}_{u,v}\|^2-\|\boldsymbol{G}\boldsymbol{\Lambda}\boldsymbol{x}_{l,s}-\boldsymbol{G}\boldsymbol{x}_{l,s}\|^2}{\sqrt{2}\sigma_E\|\boldsymbol{G}\boldsymbol{x}_{l,s}-\boldsymbol{G}\boldsymbol{x}_{u,v}\|}\right). \tag{16}$$

Finally, through substituting (16) into (14), the ABEP union bound of Eve can be computed.

3.2 Secrecy rate analysis

In this subsection, we continue to analyze the secrecy rate of the proposed DM-DRS scheme in the context of the discrete input signal for both the traditional APM symbols and the distributed receiver selection mapping symbols, as well as the continuous output symbols.

According to [21], the secrecy rate R_S is the difference between Bob's ergodic rate R_B and Eve's ergodic rate R_E, while it is always non-negative. Thus, the secrecy rate is formed as

$$R_S=[R_B-R_E]^+, \tag{17}$$

where $[a]^+=\max\{0,a\}$. Let us now respectively formulate the expressions of R_B and R_E.

Firstly, based on [19], Bob's ergodic rate R_B is given by

$$R_B=\log_2|\mathcal{X}|-\underbrace{\frac{1}{|\mathcal{X}|}\sum_{\boldsymbol{x}_{l,s}\in\mathcal{X}}\mathbb{E}_{\boldsymbol{n}}\left[\log_2\left(\sum_{\boldsymbol{x}_{u,v}\in\mathcal{X}}\exp(\Psi)\right)\right]}_{A}, \tag{18}$$

where we have

$$\Psi=\frac{-\|\boldsymbol{H}_{\boldsymbol{\Lambda}}(\boldsymbol{x}_{l,s}-\boldsymbol{x}_{u,v})+\boldsymbol{n}\|^2+\|\boldsymbol{n}\|^2}{\sigma_n^2}. \tag{19}$$

More specially, in the following expression—for the sake of simplicity—we assume that Bob and Eve receive the same noise power, i.e., $\sigma_n^2=\sigma_E^2$, where $\sigma_n^2=\frac{1}{\beta_s}$, in which β_s is the average SNR per symbol. When SNR is sufficiently high, the term A tends to be zero, and Bob reaches its ergodic rate upper bound of $\log_2|\mathcal{X}|$.

Table 1 System parameters

Figure	Scheme	N_u	M	Λ	N_e	Θ_E	SNR
1	DM-DRS	2	4	$\mathrm{diag}\{e^{j0\pi}, e^{j0\pi}, e^{j0\pi}, e^{j0\pi}\}$, $\mathrm{diag}\{e^{j7\pi/45}, e^{j8\pi/45}, e^{j2\pi/9}, e^{j\pi/4}\}$	4	$\{20°, 60°, 110°, 230°\}$	–
2	DM-CR	–	4	$\mathrm{diag}\{e^{j7\pi/45}, e^{j8\pi/45}, e^{j2\pi/9}, e^{j\pi/4}\}$	–	–	–
	SDM	1	4	$\mathrm{diag}\{e^{j7\pi/45}, e^{j8\pi/45}, e^{j2\pi/9}, e^{j\pi/4}\}$	–	–	–
	DM-DRS	2	4	$\mathrm{diag}\{e^{j7\pi/45}, e^{j8\pi/45}, e^{j2\pi/9}, e^{j\pi/4}\}$	–	–	–
3	DM-CR	–	64	$\mathrm{diag}\{e^{j7\pi/45}, e^{j8\pi/45}, e^{j2\pi/9}, e^{j\pi/4}\}$	–	–	–
	SDM	1	16	$\mathrm{diag}\{e^{j7\pi/45}, e^{j8\pi/45}, e^{j2\pi/9}, e^{j\pi/4}\}$	–	–	–
	DM-DRS	2	4	$\mathrm{diag}\{e^{j7\pi/45}, e^{j8\pi/45}, e^{j2\pi/9}, e^{j\pi/4}\}$	–	–	–
4	DM-CR	–	4, 16	$\mathrm{diag}\{e^{j7\pi/45}, e^{j8\pi/45}, e^{j2\pi/9}, e^{j\pi/4}\}$	1	–	10 dB
	SDM	1	4, 16	$\mathrm{diag}\{e^{j7\pi/45}, e^{j8\pi/45}, e^{j2\pi/9}, e^{j\pi/4}\}$	1	–	10 dB
	DM-DRS	2	4, 16	$\mathrm{diag}\{e^{j7\pi/45}, e^{j8\pi/45}, e^{j2\pi/9}, e^{j\pi/4}\}$	1	–	10 dB
5, 6	DM-DRS	1, 2, 3	4	$\mathrm{diag}\{e^{j7\pi/45}, e^{j8\pi/45}, e^{j2\pi/9}, e^{j\pi/4}\}$	4	$\{20°, 60°, 110°, 230°\}$	–
7	DM-CR	–	4	$\mathrm{diag}\{e^{j7\pi/45}, e^{j8\pi/45}, e^{j2\pi/9}, e^{j\pi/4}\}$	1	$15°$	–
	SDM	1	4	$\mathrm{diag}\{e^{j7\pi/45}, e^{j8\pi/45}, e^{j2\pi/9}, e^{j\pi/4}\}$	1	$15°$	–
	DM-DRS	2	4	$\mathrm{diag}\{e^{j7\pi/45}, e^{j8\pi/45}, e^{j2\pi/9}, e^{j\pi/4}\}$	1	$15°$	–
8	DM-DRS	2	4	$\mathrm{diag}\{e^{j7\pi/45}, e^{j8\pi/45}, e^{j2\pi/9}, e^{j\pi/4}\}$	1, 2, 3, 4, 5	$\{20°, 60°, 110°, 230°, 170°\}$	–

Secondly, in order to evaluate Eve's ergodic rate, we consider the worst case that the scrambling matrix is attained by Eve. That is, Eve is capable of realizing the maximum ergodic rate in this case. Similar to Bob's ergodic rate, we can write Eve's ergodic rate as

$$R_E = \log_2 |\mathcal{X}| - \underbrace{\frac{1}{|\mathcal{X}|} \sum_{\boldsymbol{x}_{l,s} \in \mathcal{X}} \mathbb{E}_{\boldsymbol{n}_E} \left[\log_2 \left(\sum_{\boldsymbol{x}_{u,v} \in \mathcal{X}} \exp(\Phi) \right) \right]}_{B}, \tag{20}$$

where we have

$$\Phi = \frac{-\|\boldsymbol{G}\boldsymbol{\Lambda}(\boldsymbol{x}_{l,s} - \boldsymbol{x}_{u,v}) + \boldsymbol{n}_E\|^2 + \|\boldsymbol{n}_E\|^2}{\sigma_E^2}. \tag{21}$$

Naturally, the term B tends to be zero, and Eve reaches its ergodic rate upper bound of $\log_2 |\mathcal{X}|$ at the high SNR region.

Therefore, the secrecy rate of the proposed DM-DRS scheme can be computed as

$$R_S = \left[\frac{1}{|\mathcal{X}|} \mathbb{E}_{\boldsymbol{n},\boldsymbol{n}_E} \sum_{\boldsymbol{x}_{l,s} \in \mathcal{X}} \log_2 \left(\sum_{\boldsymbol{x}_{u,v} \in \mathcal{X}} \frac{\exp(\Phi)}{\exp(\Psi)} \right) \right]^+. \tag{22}$$

Obviously, since the secrecy rate is the difference between Bob's and Eve's ergodic rates, it tends to be zero when SNR is sufficiently high. Particularly, we only use the Monte Carlo simulations to investigate the secrecy rate, because it is difficult to obtain the closed-form solution of the DM-DRS scheme.

4 Numerical results

In this section, numerical results are presented to highlight the advantage of the proposed DM-DRS scheme over both additive white gaussian noise (AWGN) and free space channel, where the BER and secrecy rate are characterized. For comparison, the performances of the traditional DM-CR and SDM schemes are also considered. Moreover, we assume that Alice employs $N_t = 10$ phased array antennas, with antenna spacing $d = \lambda/4$. Bob employs $N_r = 4$ single-antenna receivers, with a direction set $\Theta_B = \{15°, 85°, 120°, 210°\}$. The other parameters are listed in Table 1, where the corresponding set of Eve's N_e directions in Figure 8 is formed from the front N_e values of Θ_E, when the different number of Eve's receivers is considered.

In Figure 1, we compare Bob's and Eve's theoretical and simulated BER performances of the proposed DM-DRS scheme with ($\boldsymbol{\Lambda} = \mathrm{diag}\{e^{j7\pi/45}, e^{j8\pi/45}, e^{j2\pi/9}, e^{j\pi/4}\}$) and without ($\boldsymbol{\Lambda} = \mathrm{diag}\{e^{j0\pi}, e^{j0\pi}, e^{j0\pi}, e^{j0\pi}\}$) the scrambling matrix $\boldsymbol{\Lambda}$. From the results, we can draw the following straightforward observations.

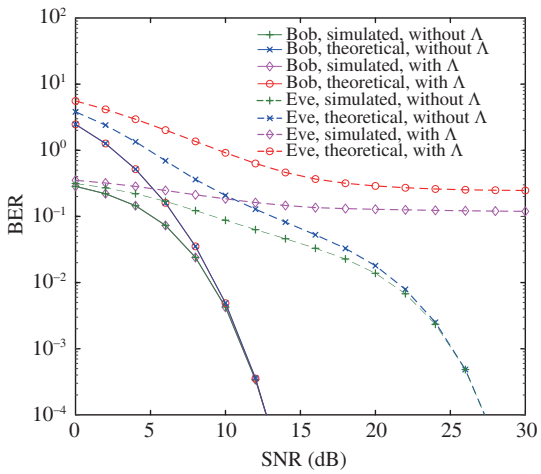

Figure 1 (Color online) Bob's and Eve's theoretical and simulated BER performances of the proposed DM-DRS scheme with and without the scrambling matrix $\mathbf{\Lambda}$.

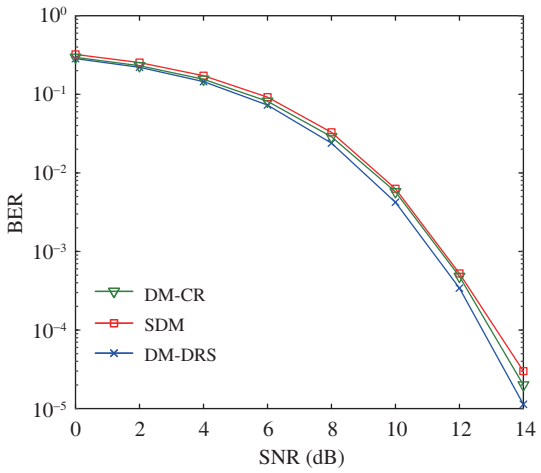

Figure 2 (Color online) Bob's BER performances of our DM-DRS scheme in comparison to the traditional DM-CR and SDM counterparts.

When SNR is sufficiently high, the theoretical curve forms tight upper bound of the simulated curve for the proposed DM-DRS scheme at both Bob and Eve in the case without $\mathbf{\Lambda}$. Meanwhile, the theoretical upper bound of Bob is reachable and that of Eve is close to the simulated results in the case with $\mathbf{\Lambda}$ as the SNR increases. This verifies the theoretical ABEP analysis of (11) and (14) from upper bounds toward the simulated results. On the other hand, in the case without $\mathbf{\Lambda}$, we can see that Bob has the advantage of providing an SNR gain about 14 dB over Eve at a BER of 10^{-4}, owing to the difference between Bob's and Eve's channels, and then the power received by Eve will be lower than that of Bob. Note that, although the BER performance of Eve without $\mathbf{\Lambda}$ is worse than that of Bob, it may correctly recover the information when Eve is enough sensitive. Specially, comparing to the proposed DM-DRS scheme without $\mathbf{\Lambda}$, Eve's BER performance is seriously degraded owing to the effect of $\mathbf{\Lambda}$, while Bob's BER performance is not affected. This is because that $\mathbf{\Lambda}$ is known at Bob but difficultly known at Eve. Therefore, owing to the introduction of $\mathbf{\Lambda}$, the proposed DM-DRS scheme is capable of improving security.

Figure 2 compares Bob's BER performances of the proposed DM-DRS scheme to its traditional counterparts, where both the simulated DM-CR and SDM schemes are described. As shown in Figure 2, our proposed DM-DRS scheme exhibits a lower BER than that of the traditional DM-CR and SDM schemes. More explicitly, at one transmission, we use QPSK to transmit the data streams, and thus there are 2 and 4 bits respectively transmitted in traditional DM-CR and SDM schemes under the setting of $N_r = 4$, while the proposed DM-DRS scheme can transmit 6 bits under the setting of $N_r = 4$ and $N_u = 2$. This is owing to the fact that compared with traditional DM-CR, despite the same data streams conveyed by APM symbols, and extra data streams conveyed by the index of cooperative receivers in traditional SDM, it is still with low transmission rate in comparison to the proposed DM-DRS scheme, where the multiple data streams are simultaneously conveyed by APM symbols, in addition to the data stream mapping of index combination. Based on the above comparative results, we can infer that DM-DRS can effectively improve the transmission rate than traditional DM-CR and SDM, in addition to an improved BER performance.

Figure 3 shows Bob's comparative BER results among DM-CR, SDM and DM-DRS from another perspective, where we assume one block of 6 bits is transmitted at one transmission. Naturally, the proposed DM-DRS scheme just needs to employ QPSK modulation with the aid of receiver subset selection. While the traditional DM-CR scheme employs 64 orthogonal amplitude modulation (QAM) owing to its inherent drawback that the information is transmitted only by traditional APM technique, which brings higher computational complexity and worse BER performance. Naturally, as for the traditional SDM scheme, 16QAM is employed, this also results in the bad BER performance in comparison to DM-DRS. Totally, Figures 2 and 3 imply that the proposed DM-DRS scheme outperforms traditional DM-CR and SDM schemes in terms of BER performance.

Figure 4 shows Eve's BER performances of both the proposed DM-DRS scheme and its traditional DM-

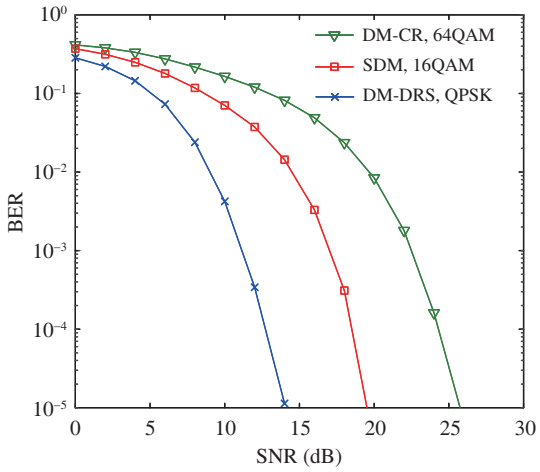

Figure 3 (Color online) Bob's BER performances, where our DM-DRS scheme transmits the same 6 bits as traditional DM-CR and SDM.

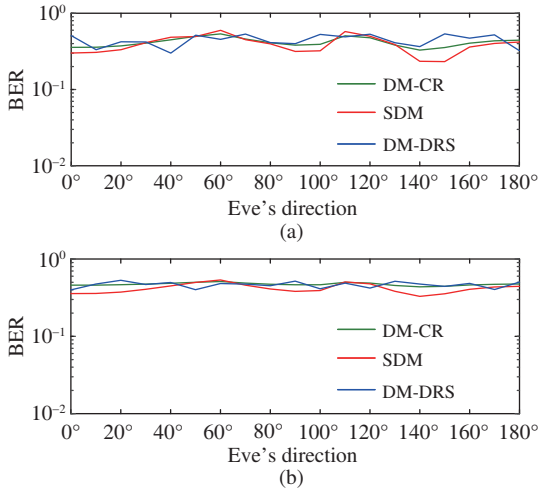

Figure 4 (Color online) Eve's BER performances, (a) one symbol adopts QPSK, (b) another symbol adopts 16QAM.

CR and SDM counterparts against Eve's direction. For the proposed DM-DRS scheme, assuming random QPSK symbols are transmitted to one receiver, while random 16QAM symbols to another receiver. As shown in Figure 4(a), we take the QPSK symbols into account, and the DM-DRS curve exhibits poor BER result, which is close to traditional DM-CR and SDM. Furthermore, these observations in Figure 4(b) are completely consistent with those in Figure 4(a). In Figure 4(b), we consider the 16QAM symbols, particularly, the BER gaps among the proposed DM-DRS scheme and traditional DM-CR and SDM are almost negligible. Hence, the security performance can be guaranteed in terms of Eve's BER performance of our proposed DM-DRS scheme.

Figure 5 shows Bob's and Eve's BER performances of the proposed DM-DRS scheme in the context of different numbers of activated receivers N_u. From the result of Figure 5, an important observation is that, given the QPSK modulation and SNR per bit, there exists an optimal value of N_u, which reflects the optimal Bob's BER performance. Particularly, when $N_u = 2$ and $N_u = 3$, Bob's BER performance of the proposed DM-DRS scheme outperforms that of $N_u = 1$, in addition to 2 and 4 more bits transmitted. Furthermore, it also suggests in Figure 5 that as SNR increases, the larger number of activated receivers is, the worse Eve's BER performance will be. Note that, Eve's BER performance is prohibitively poor regardless of the value of N_u. This implies the DM-DRS scheme has the advantage of guaranteeing the security, owing to the effect of the scrambling matrix.

Figure 6 shows the attainable ergodic rates of both Bob and Eve for different numbers of activated receivers N_u, as well as the secrecy rate of the proposed DM-DRS. It can be seen in Figure 6 that at a given QPSK modulation, both Bob's and Eve's ergodic rate curves with $N_u = 1, 2, 3$ reach the upper bound of 4, 6, 8, respectively, and these results are in correspondence with the analysis of the ergodic rate upper bound of $\log_2 |\mathcal{X}|$ in (18) and (20) at the sufficiently high SNR. Furthermore, for a given N_u, the secrecy rate curve initially increases until it reaches a peak, and then decreases to zero, this corresponds with the analysis of (22) at the high SNR region. To be specific, in order to guarantee the transmission security, in other words, when the secrecy rate is guaranteed to be positive, we may set SNR at the low and medium regions for dealing with the worst situation the scrambling matrix is known at Eve.

Figure 7 compares Bob's and Eve's ergodic rates as well as the secrecy rate of the proposed DM-DRS scheme and its traditional DM-CR and SDM counterparts, where Eve is equipped with single-antenna receiver. When the SNR increases, for traditional DM-CR, SDM and DM-DRS, the ergodic rates of Bob are respectively bounded as 2, 4, 6 ($\log_2 M$, $\log_2 (MN_r)$, $\log_2 |\mathcal{X}|$) bits/s/Hz and that of Eve are respectively bounded as 2, 2, 6 ($\log_2 M$, $\log_2 M$, $\log_2 |\mathcal{X}|$) bits/s/Hz under the setting of $\{M, N_r, N_u\} = \{4, 4, 2\}$. Obviously, both Bob and Eve achieve the maximum ergodic rates in the proposed DM-DRS scheme. On the other hand, for each scheme, the secrecy rate always first increases to a peak value, and then decreases to a stable value. Specially, under the worst case that the scrambling factor is known at Eve, the secrecy rate performance of DM-CR is always the worst in the entire SNR region,

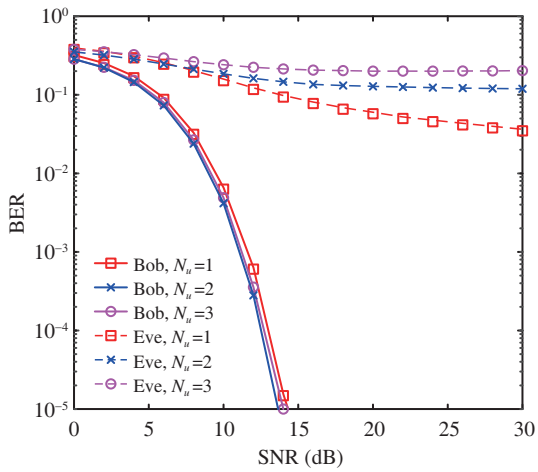

Figure 5 (Color online) Bob's and Eve's BER performances of the proposed DM-DRS versus different N_u.

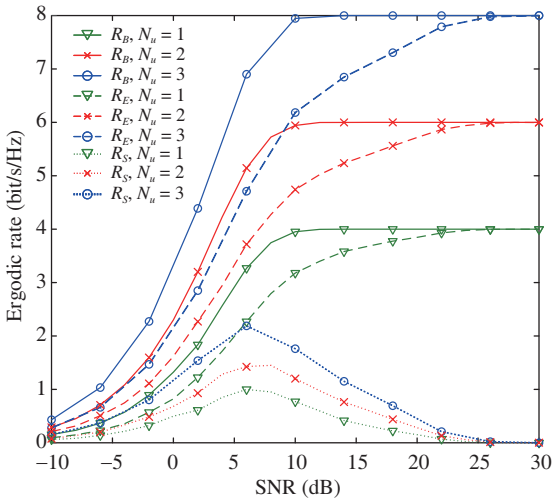

Figure 6 (Color online) Bob's and Eve's ergodic rates as well as the secrecy rate of the proposed DM-DRS versus different N_u.

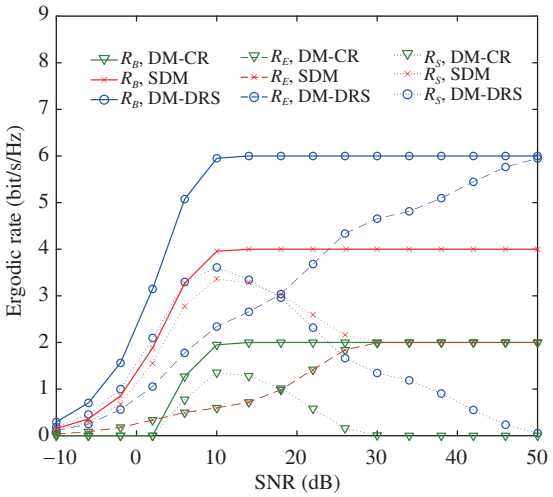

Figure 7 (Color online) Bob's and Eve's ergodic rates as well as the secrecy rate of the proposed DM-DRS scheme and its traditional DM-CR and SDM counterparts.

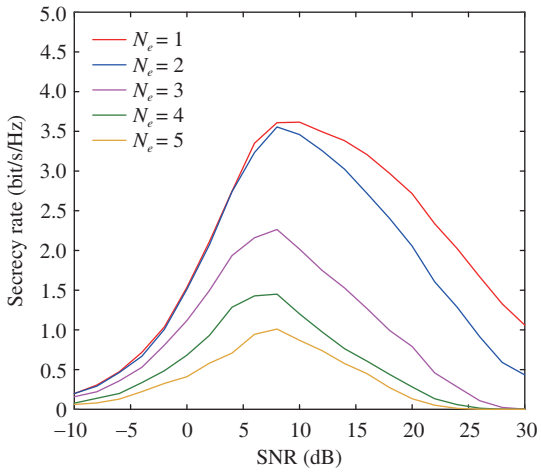

Figure 8 (Color online) Secrecy rates of the proposed DM-DRS versus different N_e.

where the information is transmitted by APM symbols. Moreover, one data stream is transmitted by the index of Bob's cooperative receivers, in addition to traditional digital modulation in SDM. However, it may be unpractical to assume that Eve cannot detect the index information, which results in that the secrecy rate maintains a stable value of 2 ($\log_2 N_r$) as SNR $\to \infty$. For the proposed DM-DRS scheme, hence it is more reasonable to assume that joint demodulation of the receiver selection and APM symbols is employed at Eve. Furthermore, it achieves the best secrecy rate performance in the low and medium SNR regions.

Figure 8 shows the secrecy rate of the proposed DM-DRS scheme for different numbers of Eve's distributed receivers N_e. From Figure 8, it can be observed that the setup of fewer distributed receivers N_e exhibits a higher secrecy rate at a given SNR gain. This is owing to the fact that more distributed receivers lead to the transmission information more vulnerable to eavesdropping. In addition, the fewer number of N_e is, the higher SNR gain will be for Eve to reach the upper bound of ergodic rate. Since the secrecy rate is the difference between Bob's and Eve's ergodic rates, the larger SNR interval is desired to realize the positive secrecy rate.

5 Conclusion

In summary, in this contribution, the BER and secrecy rate performances of the proposed DM-DRS scheme have been investigated and compared with its traditional DM-CR and SDM counterparts. We introduced the detailed process of the DM-DRS scheme, derived a theoretical upper-bound analysis of Bob's and Eve's average BER, and quantified the secrecy rate. By contrast, we can conclude that the proposed scheme has an improved performance than DM-CR and SDM. More specifically, in addition to the improved transmission rate, the proposed DM-DRS scheme is capable of obtaining improved BER performance, while achieving the best secrecy rate performance in the low and medium SNR regions. Furthermore, we showed there exists the optimal number of the activated receivers in terms of legitimate user's BER performance. As for the eavesdropper, the BER performance is prohibitively poor, and the security of information transmission can be guaranteed. On the other hand, when the SNR is sufficiently high, both Bob and Eve are capable of reaching the upper bound of ergodic rate, and the secrecy rate tends to be zero. However, when the number of Eve's receivers decreases, the SNR interval for achieving a positive secrecy rate becomes large.

Acknowledgements This work was supported by National Key R&D Program of China (Grant No. 2018YFB1800800), National Natural Science Foundation of China (Grant No. 61671131), Project from the Science and Technology on Communication Networks Laboratory, and the 54th Research Institute of China Electronics Technology Group Corporation (CETC) (Grant No. 6142104180407).

References

1 Yang N, Wang L F, Geraci G, et al. Safeguarding 5G wireless communication networks using physical layer security. IEEE Commun Mag, 2015, 53: 20–27
2 Zou Y L, Zhu J, Wang X B, et al. A survey on wireless security: technical challenges, recent advances, and future trends. Proc IEEE, 2016, 104: 1727–1765
3 Qi Q, Chen X M, Zhong C J, et al. Physical layer security for massive access in cellular Internet of Things. Sci China Inf Sci, 2020, 63: 121301
4 Wang H M, Luo M, Yin Q, et al. Hybrid cooperative beamforming and jamming for physical-layer security of two-way relay networks. IEEE Trans Inform Forensic Secur, 2013, 8: 2007–2020
5 Lu Z Y, Sun L L, Zhang S, et al. Optimal power allocation for secure directional modulation networks with a full-duplex UAV user. Sci China Inf Sci, 2019, 62: 080304
6 Zhuang Z H, Xu L, Li J Y, et al. Machine-learning-based high-resolution DOA measurement and robust directional modulation for hybrid analog-digital massive MIMO transceiver. Sci China Inf Sci, 2020, 63: 180302
7 Babakhani A, Rutledge D B, Hajimiri A. Transmitter architectures based on near-field direct antenna modulation. IEEE J Solid-State Circ, 2008, 43: 2674–2692
8 Daly M P, Bernhard J T. Directional modulation technique for phased arrays. IEEE Trans Antenna Propagat, 2009, 57: 2633–2640
9 Valliappan N, Lozano A, Heath R W. Antenna subset modulation for secure millimeter-wave wireless communication. IEEE Trans Commun, 2013, 61: 3231–3245
10 Alotaibi N N, Hamdi K A. Switched phased-array transmission architecture for secure millimeter-wave wireless communication. IEEE Trans Commun, 2016, 64: 1303–1312
11 Ding Y, Fusco V F. A vector approach for the analysis and synthesis of directional modulation transmitters. IEEE Trans Antenna Propagat, 2014, 62: 361–370
12 Ding Y, Fusco V F. Orthogonal vector approach for synthesis of multi-beam directional modulation transmitters. Antenn Wirel Propag Lett, 2015, 14: 1330–1333
13 Xiao Y P, Tang W P, Xiao Y, et al. Directional modulation with cooperative receivers. IEEE Access, 2018, 6: 34992–35000
14 You Q, Xiao Y P. Spatial and directional modulation with scrambling. Phys Commun, 2019, 35: 100694
15 Mesleh R Y, Haas H, Sinanovic S, et al. Spatial modulation. IEEE Trans Veh Technol, 2008, 57: 2228–2241
16 Yang P, Renzo M D, Xiao Y, et al. Design guidelines for spatial modulation. IEEE Commun Surv Tut, 2015, 17: 6–26
17 Jiang X Q, Wen M W, Hai H, et al. Secrecy-enhancing scheme for spatial modulation. IEEE Commun Lett, 2018, 22: 550–553
18 Zhang R, Yang L L, Hanzo L. Generalised pre-coding aided spatial modulation. IEEE Trans Wirel Commun, 2013, 12: 5434–5443
19 Zhang R, Yang L L, Hanzo L. Error probability and capacity analysis of generalised pre-coding aided spatial modulation. IEEE Trans Wirel Commun, 2015, 14: 364–375
20 Zheng J P. Fast receive antenna subset selection for pre-coding aided spatial modulation. IEEE Wirel Commun Lett, 2015, 4: 317–320
21 Bloch M, Barros J, Rodrigues M R D, et al. Wireless information-theoretic security. IEEE Trans Inform Theor, 2008, 54: 2515–2534